

# Characterization of a hyperpolarization-activated time-dependent potassium current in canine cardiomyocytes from pulmonary vein myocardial sleeves and left atrium

Joachim R. Ehrlich<sup>1,2</sup>, Tae-Joon Cha<sup>1,2</sup>, Liming Zhang<sup>1,2</sup>, Denis Chartier<sup>1,2</sup>, Louis Villeneuve<sup>1</sup>, Terence E. Hébert<sup>2,3</sup> and Stanley Nattel<sup>1,2,4</sup>

Departments of <sup>1</sup>Medicine and <sup>3</sup>Anaesthesiology, University of Montreal; <sup>4</sup>Department of Pharmacology and Therapeutics, McGill University, and <sup>2</sup>Research Center, Montreal Heart Institute, Montreal, Quebec, Canada

Cardiomyocytes from the pulmonary vein sleeves (PVs) are known to play an important role in atrial fibrillation. PVs have been shown to exhibit time-dependent hyperpolarization-induced inward currents of uncertain nature. We observed a time-dependent  $K^+$  current upon hyperpolarization of PV and left atrial (LA) cardiomyocytes ( $I_{KH}$ ) and characterized its biophysical and pharmacological properties. The activation time constant was weakly voltage dependent, ranging from  $386 \pm 14$  to  $427 \pm 37$  ms between  $-120$  and  $-90$  mV, and the half-activation voltage averaged  $-93 \pm 4$  mV.  $I_{KH}$  was larger in PV than LA cells (e.g. at  $-120$  mV:  $-2.8 \pm 0.3$  versus  $-1.9 \pm 0.2$  pA pF<sup>-1</sup>, respectively,  $P < 0.01$ ). The reversal potential was  $\sim -84$  mV with  $5.4$  mM  $[K^+]_o$  and changed by  $55.7 \pm 2.4$  mV per decade  $[K^+]_o$  change.  $I_{KH}$  was exquisitely  $Ba^{2+}$  sensitive, with a 50% inhibitory concentration ( $IC_{50}$ ) of  $2.0 \pm 0.3$   $\mu$ M (versus  $76.0 \pm 17.9$   $\mu$ M for instantaneous inward-rectifier current,  $P < 0.01$ ), and showed similar  $Cs^+$  sensitivity to instantaneous current.  $I_{KH}$  was potently blocked by tertiapin-Q, a selective Kir3-subunit channel blocker ( $IC_{50}$   $10.0 \pm 2.1$  nM), was unaffected by atropine and was significantly increased by isoproterenol (isoprenaline), carbachol and the non-hydrolysable guanosine triphosphate analogue GTP $\gamma$ S.  $I_{KH}$  activation by carbachol required GTP in the pipette and was prevented by pertussis toxin pretreatment. Tertiapin-Q delayed repolarization in atropine-exposed multicellular atrial preparations studied with standard microelectrodes (action potential duration pre- versus post-tertiapin-Q:  $190.4 \pm 4.3$  versus  $234.2 \pm 9.9$  ms, PV;  $202.6 \pm 2.6$  versus  $242.7 \pm 6.2$  ms, LA; 2 Hz,  $P < 0.05$  each). Seven-day atrial tachypacing significantly increased  $I_{KH}$  (e.g. at  $-120$  mV in PV: from  $-2.8 \pm 0.3$  to  $-4.5 \pm 0.5$  pA pF<sup>-1</sup>,  $P < 0.01$ ). We conclude that  $I_{KH}$  is a time-dependent, hyperpolarization-activated  $K^+$  current that likely involves Kir3 subunits and appears to play a significant role in atrial physiology.

(Resubmitted 13 January 2004; accepted after revision 12 March 2004; first published online 12 March 2004)

**Corresponding author** S. Nattel: Research Center, Montreal Heart Institute, 5000 Belanger Street E, Montreal, Quebec, Canada H1T 1C8. Email: nattel@icm.umontreal.ca

Cardiac tissue in the pulmonary vein sleeves (PVs) are important for the initiation and maintenance of atrial fibrillation (AF) (Haissaguerre *et al.* 1998; Pappone *et al.* 2000). The cellular mechanisms underlying PV arrhythmogenicity remain obscure. Enhanced automaticity and triggered activity have been reported in isolated PV sleeve cardiomyocytes (Chen *et al.* 2001). PVs were found to show a time-dependent hyperpolarization-activated current that was increased by atrial tachycardia (AT), which was not characterized but was believed to represent  $I_f$  (Chen *et al.* 2001). In

previous studies of PV ionic properties (Ehrlich *et al.* 2003), we indeed observed hyperpolarization-activated inward currents, but found them to be highly sensitive to  $Ba^{2+}$ , a pharmacological property inconsistent with  $I_f$  (DiFrancesco, 1993). We therefore designed the present study to characterize this current in terms of its kinetics, ionic selectivity, pharmacological response and potential functional role. Based on evidence (see below) that the current is carried predominantly by  $K^+$ , we will refer to it as  $I_{KH}$  for hyperpolarization-induced  $K^+$  current.

## Methods

### Tissue and cell preparations

Adult mongrel dogs of either sex (20–35 kg) were anaesthetized with pentobarbital (30 mg kg<sup>-1</sup> i.v.) and artificially ventilated with room air. Hearts and adjacent lung tissue were quickly excised through a left lateral thoracotomy and immersed in oxygenated Tyrode solution (composition below) at room temperature. Removal of the heart and lungs produced circulatory arrest, resulting in effective and humane killing. A left atrial (LA) preparation with the PVs intact was perfused via the left circumflex coronary artery, and subjected to either standard fine-tipped microelectrode recording of action potentials (APs) or cardiomyocyte isolation with collagenase-containing solutions, as previously described (Ehrlich *et al.* 2003). Six dogs were subjected to atrial tachycardia-induced remodelling induced by 1 week of atrial pacing at 400 beats min<sup>-1</sup> after ablation of the AV node, as previously described (Li *et al.* 1999). All animal care and handling procedures followed the guidelines of the Canadian Council on Animal Care.

To isolate LA and PV cardiomyocytes, the proximal circumflex artery was cannulated and the distal ends of PV myocardial sleeves (approximately 1–1.5 cm from the PV–LA junction) were marked with silk thread prior to subsequent enzyme perfusion with collagenase (100 U ml<sup>-1</sup>, Worthington, type II), in order to facilitate localization of PV sleeves after enzymatic digestion. After a period of ~45 min, epicardial tissue was removed and the underlying muscular sleeve of PVs was found to be well digested, with the smooth muscle layer still intact and unaffected by the isolation procedure. With this method, PVs were well-perfused and single cardiomyocytes could be isolated from all veins. Cardiomyocytes obtained from PVs were morphologically similar to LA cardiomyocytes isolated from the LA free wall in the same dogs. All comparisons were based on PV and LA cardiomyocytes isolated from each dog on each experimental day. After isolation, cells were stored at 4°C and studied on the same day. For standard microelectrode experiments, intact tissue preparations including the LA and adjacent PVs were mounted in a chamber and perfused via the circumflex artery with oxygenated Krebs solution at 36 ± 0.5°C (Kneller *et al.* 2002).

### Electrophysiology

Currents were recorded with the whole-cell patch-clamp technique at 36 ± 0.5°C, as previously described (Yue *et al.* 1996). All junction potentials were zeroed prior

to formation of gigaohm seals. The compensated series resistance and capacitive time constant ( $\tau$ ) averaged 3.9 ± 0.1 M $\Omega$  and 257 ± 81  $\mu$ s, respectively, and voltage errors across the series resistance did not exceed 5 mV. Capacitance was assessed using 5 mV, 10 ms hyperpolarizing steps from a holding potential (HP) of -60 mV. Junction potentials averaged 11.8 ± 0.9 mV and were not routinely corrected. Cell capacitance averaged 81 ± 4 pF for PV and 69 ± 8 pF for LA cardiomyocytes ( $n = 83$ , 29 cells, respectively,  $P = \text{n.s.}$ ). Atrial tachycardia did not affect cell capacitance (84 ± 10 versus 91 ± 10 pF,  $n = 9$  and 12 for PV and LA cells, respectively,  $P = \text{n.s.}$ ). Original recordings are shown in terms of current amplitude, but mean data are presented as current density (pA pF<sup>-1</sup>) to control for variability in cell size.

Currents were recorded with hyperpolarizing and depolarizing pulses (generally 4 s duration) from a HP of -40 mV to selected test potentials (TPs). Recordings were repeated 3 times, and mean values obtained. For the determination of reversal potentials, tail currents were recorded after 1.6 s pulses to -120 mV followed by 3.2 s depolarizations to TPs between -110 and +20. All voltage protocols were delivered at 0.1 Hz.

Fine-tipped microelectrodes (resistance 15–20 M $\Omega$  when filled with 3 M KCl) coupled to a high input-impedance amplifier were used to record APs as previously described (Kneller *et al.* 2002).

### Solutions

Tyrode solution contained (mM): NaCl 136, KCl 5.4, MgCl<sub>2</sub> 1, CaCl<sub>2</sub> 1, NaH<sub>2</sub>PO<sub>4</sub> 0.33, Hepes 5 and dextrose 10 (pH 7.35 with NaOH). The cell-storage solution contained (mM): KCl 20, KH<sub>2</sub>PO<sub>4</sub> 10, dextrose 10, mannitol 40, L-glutamic acid 70,  $\beta$ -OH-butyric acid 10, taurine 20, EGTA 10 and 0.1% bovine serum albumin (pH 7.3, KOH). Nifedipine (5  $\mu$ M) was used to suppress L-type Ca<sup>2+</sup> current ( $I_{Ca}$ ) in all experiments. 4-Aminopyridine (4-AP, 2 mM) was added to suppress transient outward current ( $I_{to}$ ). Atropine was added as indicated to the extracellular solution to suppress muscarinic receptor-activated currents. Na<sup>+</sup> current ( $I_{Na}$ ) contamination was avoided by using a HP of -40 mV for recording of hyperpolarization-induced currents and by substitution of equimolar Tris-HCl for external NaCl for tail-current recordings. When different external K<sup>+</sup> concentrations were applied, the osmolarity was kept constant by proportionate reduction of NaCl content in the solution. The standard internal solution contained (mM): potassium aspartate 110, KCl 20, MgCl<sub>2</sub> 1, MgATP 5, GTP (lithium salt) 0.1, Hepes 10, sodium phosphocreatine 5 and EGTA 5.0 (pH 7.3 with KOH). In experiments with K<sup>+</sup>-free

internal solution, potassium aspartate was replaced by equimolar caesium aspartate and KCl by CsCl and pH was set to 7.3 with CsOH. For standard-microelectrode experiments, a solution containing (mM): NaCl 120, KCl 4,  $\text{KH}_2\text{PO}_4$  1.2,  $\text{MgSO}_4$  1.2,  $\text{NaHCO}_3$  25,  $\text{CaCl}_2$  1.25 and dextrose 5 (95%  $\text{O}_2$ –5%  $\text{CO}_2$ , pH 7.4) was used to perfuse the tissue.

Stock solutions of  $\text{BaCl}_2$  (1 M) and CsCl (1 M) were produced initially and used throughout the experiments. Stock solution of isoproterenol was prepared under protection from light on the day of experiments and freshly prepared ascorbic acid (100  $\mu\text{M}$ ) was added in order to prevent isoproterenol oxidization. Carbachol (1  $\mu\text{M}$ ) was dissolved in Tyrode solution, tertiapin-Q in 0.1% acetic acid. GTP $\gamma\text{S}$  (0.1 mM) was used in place of GTP in internal solutions for some experiments. For experiments involving pertussis toxin (PTX, stock solution dissolved in distilled  $\text{H}_2\text{O}$ ) cells were incubated at 37°C in 1.5  $\text{mg l}^{-1}$  PTX for at least 9 h prior to experiments. Parallel controls were performed with cells from the same isolates incubated in the same fashion and the same solution, but without PTX. Vehicle alone did not affect the current. Unless otherwise specified, drugs were obtained from Sigma.

### Western blot, immunofluorescence studies and confocal imaging

After isolation of single cardiomyocytes, cells were suspended in lysis buffer (5 mM Tris pH 7.4, 2 mM EDTA, 5  $\text{mg ml}^{-1}$  trypsin inhibitor, 0.1  $\text{mg ml}^{-1}$  benzamidine, 0.43  $\text{mg ml}^{-1}$  leupeptin). After homogenization ( $2 \times 10^5$  bursts with a Polytron homogenizer) and centrifugation (20 min, 16000 r.p.m), pellets were resuspended in a buffer (75 mM Tris, 12.5 mM EDTA, 2 mM  $\text{MgCl}_2$ ). Proteins were fractionated on 7.5% SDS-PAGE gels, transferred to polyvinylidene difluoride (PVDF) membranes and blotted with anti-Kir 3.1 (1 : 1000), anti- $\text{M}_2$  receptor (1 : 500, both from Alomone), anti- $\text{G}_{\alpha i-3}$  (1 : 500, Santa Cruz) and anti-Kir 3.4 antibody (1  $\mu\text{g ml}^{-1}$ , kind gift of Dr Krapivinsky). Bands were visualized with enhanced chemiluminescence. All immunoblot band intensity measurements were normalized to the GAPDH band intensity of the loaded sample (anti-GAPDH 1 : 5000, RDI).

LA and PV cardiomyocytes were seeded on glass coverslips (prepared with 15  $\mu\text{g ml}^{-1}$  laminin) for 1 h, fixed with 2% paraformaldehyde for 20 min, washed 3 times (5 min) with phosphate-buffered saline (PBS), then blocked with 2% normal donkey serum (Jackson Laboratories) and permeabilized with 0.2% Triton X-100 for 1 h in an incubation chamber. Cells were incubated with primary antibodies (anti-Kir 3.1 1 : 200,

anti-Kir 3.2 1 : 400, both from Alomone), anti-Kir 3.4 1.3  $\mu\text{g ml}^{-1}$ ) overnight at 4°C, followed by three washes with PBS (5 min) and incubation with anti-rabbit secondary antibody (conjugated with tetra-methyl-rhodamine-isothiocyanate (TRITC)) for 1 h at room temperature, Molecular Probes). Cells were examined on an inverted laser-scanning microscope (LCM 510, Zeiss, Germany). TRITC was excited at 543 nm with a He–Ne laser and emitted fluorescence signals at 566 nm (red).

Specificity of primary antibodies for Kir 3.1, 3.2 and 3.4 was validated by immunofluorescent studies of transfected and non-transfected mammalian cells (Chinese hamster ovary cells; American Type Culture Collection, Manassas, Virginia). Transfected cells showed clear staining, whereas no staining of non-transfected cells was observed with any of the primary antibodies (not shown).

### Data analysis

Clampfit 6.0 (Axon) and Graph Pad Prism 3.0 were used for data analysis and non-linear curve fitting. Bands from immunoblots were analysed using QuantityOne software and immunofluorescence data were analysed using LSM Image Browser. Data are presented as means  $\pm$  s.e.m. and statistical comparisons were performed with Student's *t* test.  $P < 0.05$  was considered to indicate statistical significance.

## Results

### Voltage and time dependence

Upon voltage steps from  $-40$  mV,  $\sim 25\%$  of LA and PV cardiomyocytes showed instantaneous inward currents with small inactivating components and strong inward rectification typical of  $I_{K1}$  (Fig. 1A). In the remaining  $\sim 75\%$  of cells, we observed time-dependent inward currents that activated over several seconds upon hyperpolarization, with outward tail currents upon repolarization (Fig. 1B). We quantified the instantaneous current component present immediately upon resolution of the capacitive current, as well as the slow time-dependent component, which we identified with  $I_{KH}$ . When the term  $I_{KH}$  is used without additional qualification in this paper, it refers to the slowly time-dependent component. The slowly activating time-dependent current reversed at  $\sim -72$  mV ( $\sim -84$  mV with correction for the junction potential, compared to the calculated Nernst potential of  $-84.9$  mV) and showed strong inward rectification (Fig. 1C).  $I_{KH}$  was greater in PV cardiomyocytes (e.g. average at  $-120$  mV:  $-2.8 \pm 0.3$  in PV versus  $-1.9 \pm 0.2$  pA  $\text{pF}^{-1}$  in LA,  $n = 27$  and 26,

respectively,  $P < 0.01$ ), for both inward and outward (inset of Fig. 1C) components. Current activation kinetics were well-fitted by mono-exponential functions, with time constants decreasing at more negative potentials and no significant kinetic differences between LA and PV cardiomyocytes (Fig. 1D).

### Voltage dependence of activation

Tail currents recorded upon steps to  $-40$  mV after hyperpolarization to negative potentials were contaminated by activating  $\text{Na}^+$  current ( $I_{\text{Na}}$ , Fig. 2A). Replacement of extracellular NaCl with equimolar Tris-HCl eliminated the inward  $I_{\text{Na}}$  component without altering the outward current tail (Fig. 2A). For example,  $I_{\text{KH}}$  tail amplitude (determined by back-extrapolation to the onset of the pulse to  $-40$  mV) following a hyperpolarization to  $-120$  mV was  $-185 \pm 53$  pA before and  $-182 \pm 62$  pA after Tris-HCl substitution ( $n = 5$  cells studied under both conditions,  $P = \text{n.s.}$ ). Tail-current density at  $-40$  mV was a function of prepulse potential (Fig. 2B), suggesting voltage-dependent activation with a half-activation voltage ( $V_{50}$ ) of  $-93 \pm 4$  mV and a slope factor of  $-15.2 \pm 2.2$  (Boltzmann-distribution fit). Replacement of extracellular  $\text{Na}^+$  with Tris failed to significantly alter hyperpolarization-induced inward current, as illustrated in Fig. 2C and D. In five cells studied in this fashion,  $I_{\text{KH}}$  at  $-120$  mV averaged  $-3.1 \pm 0.9$  and  $-3.0 \pm 0.9$  pA  $\text{pF}^{-1}$  ( $P = \text{n.s.}$ ) in the presence and absence of extracellular  $\text{Na}^+$ , respectively. As an additional approach to analysing activation voltage dependence, we evaluated  $I_{\text{KH}}$  current-voltage data obtained as shown in Fig. 1C according to the relationship:

$$a_V = I_V / I_{\text{max}} (V - V_{\text{rev}})$$

where  $a_V$  and  $I_V$  are the activation variable and activating  $I_{\text{KH}}$  amplitude at voltage  $V$ ,  $I_{\text{max}}$  is  $I_{\text{KH}}$  amplitude at the most negative potential and  $V_{\text{rev}}$  is the reversal potential (based on tail current analyses described below). The  $V_{50}$  provided by this approach averaged  $-87 \pm 3$  mV ( $n = 10$  cells), not significantly different from the result obtained with tail current analysis. Tail currents were well-fitted by bi-exponential functions, with time constants at  $-40$  mV averaging  $243 \pm 15$  and  $1741 \pm 146$  ms and the slow component averaging  $39 \pm 2\%$  of the total.

### $\text{K}^+$ dependence and inhibition by $\text{Ba}^{2+}$ and $\text{Cs}^+$

The reversal potential of the time-dependent component (Fig. 1C:  $-72.7 \pm 1.6$  mV,  $n = 6$ ;  $\sim -84$  mV after correction for junction potential) was indicative of high  $\text{K}^+$  selectivity. With increasing  $[\text{K}^+]_{\text{ext.}}$ , tail currents reversed at increasingly positive potentials (Fig. 2E). Tail current reversal potentials were quantified by linear regression of tail currents against voltage, based on data elicited with the protocol shown in the inset in Fig. 2E. A 10-fold change in external  $\text{K}^+$  led to a  $55.7 \pm 2.4$  mV  $\text{decade}^{-1}$  shift in  $E_{\text{rev}}$  ( $n = 4$ , Fig. 2E) compared to  $61.5$  mV  $\text{decade}^{-1}$  predicted by the Nernst equation for a  $\text{K}^+$ -specific current at  $37^\circ\text{C}$ . Figure 2F and G show  $I_{\text{KH}}$  recorded in one PV cell before and after exposure to nominally  $\text{K}^+$ -free extracellular solution. In this and four other cells studied in the same fashion, elimination of extracellular  $\text{K}^+$  strongly suppressed  $I_{\text{KH}}$ . When  $I_{\text{KH}}$  was recorded with  $\text{K}^+$ -free pipette solution ( $\text{K}^+$

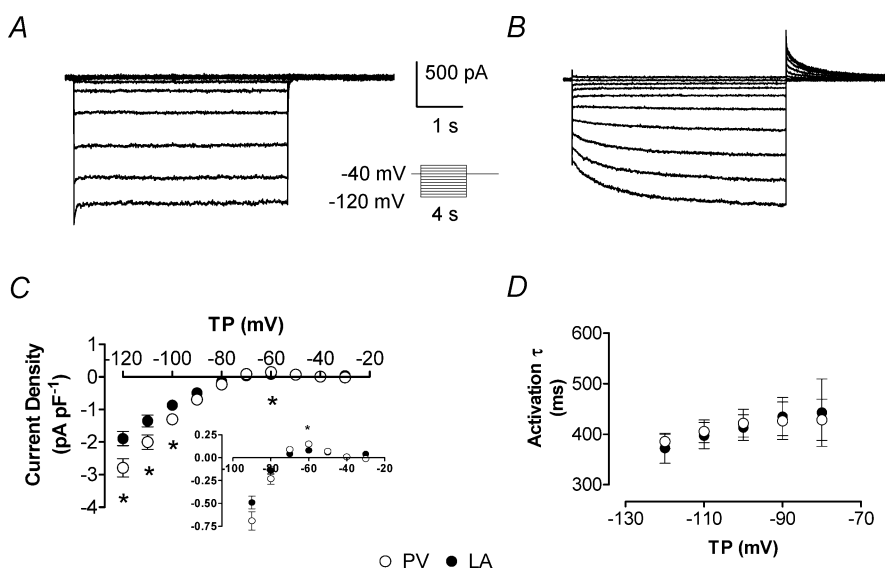


**Figure 1.**  $I_{\text{KH}}$  current characteristics

Recordings from a PV cardiomyocyte with  $I_{\text{K1}}$  and no time-dependent increasing inward component (A) and from a different PV cell (B) with clear time dependence (voltage protocol in inset). C, mean  $\pm$  s.e.m. time-dependent current ( $I_{\text{KH}}$ ) density-voltage relations in LA and PV cardiomyocytes measured at the end of a 4 s pulse.  $I_{\text{KH}}$  was significantly larger in PV ( $n = 26$  and 27 cells for LA and PV, respectively). Inset: enlargement of outward-current component that cannot be appreciated on same scale as inward currents. D, activation time constants ( $\tau$ , obtained by fitting current activation with mono-exponential functions,  $n = 10$  cells each) of  $I_{\text{KH}}$  were similar in both tissues and faster at more negative potentials.  $*P < 0.05$ ; TP, test potential; o, PV; ●, LA cardiomyocytes.

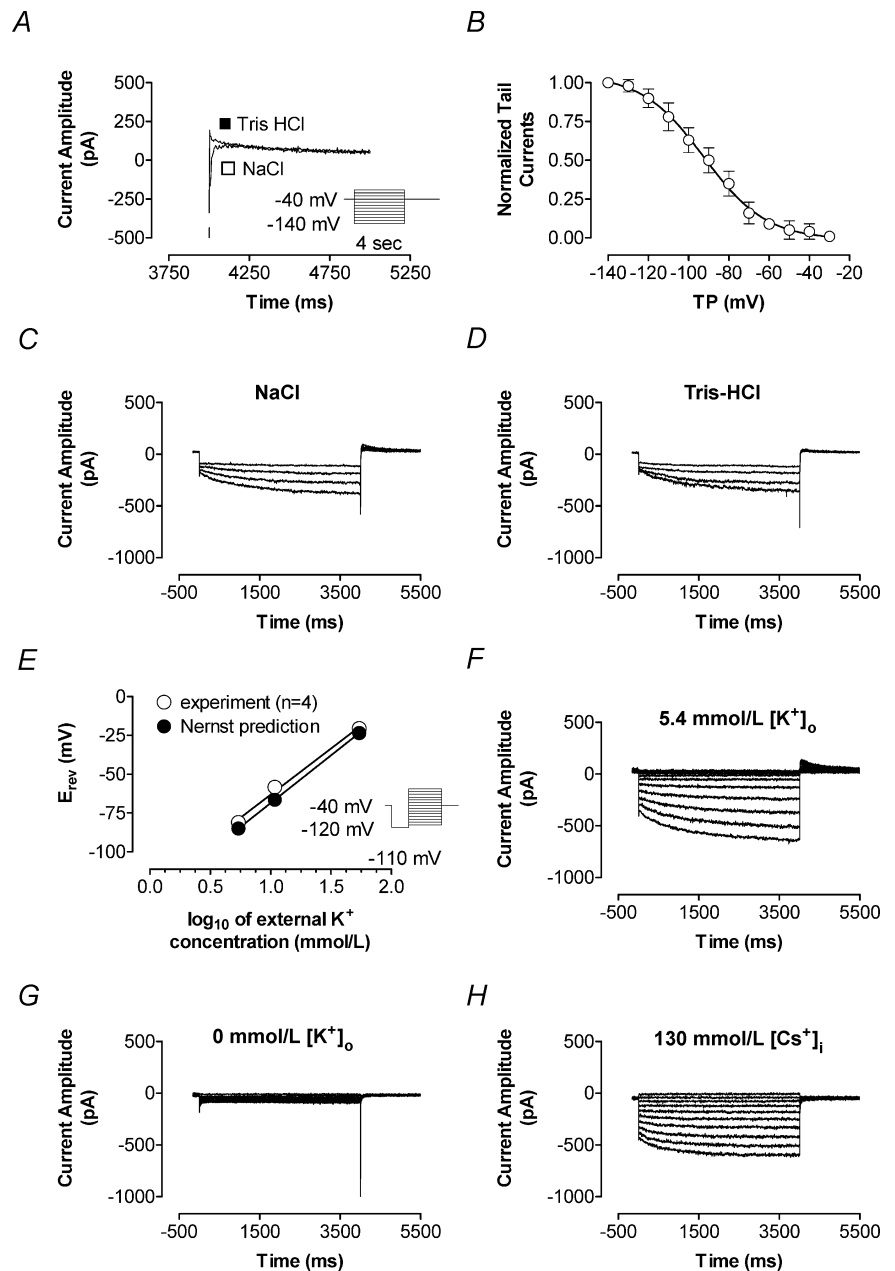
replaced by Cs<sup>+</sup>), inward current remained but outward tail currents were absent (*n* = 3, Fig. 2H).

Figure 3 illustrates the response of *I*<sub>KH</sub> to extracellular Ba<sup>2+</sup> and Cs<sup>+</sup>. Ba<sup>2+</sup> inhibited *I*<sub>KH</sub> appreciably at a concentration of 1 μM in most cells and full inhibition was generally seen at 10 μM (Fig. 3A). Mean concentration–response data for inhibition of the instantaneous component and time-dependent *I*<sub>KH</sub> are shown in Fig. 3B. Ba<sup>2+</sup> inhibited time-dependent *I*<sub>KH</sub> more potently than the instantaneous current (IC<sub>50</sub>, 76.0 ± 17.9 μM for instantaneous current versus 2.0 ± 0.3 μM for *I*<sub>KH</sub> at

–120 mV, *n* = 8 cells each, *P* < 0.01). Figure 3C shows block of *I*<sub>KH</sub> as a function of time during pulses to –120 mV in four cells. The time-dependent current was calculated at each time point as the difference between the current immediately following hyperpolarization and the current level at the time point indicated. Fractional inhibition was calculated for each time point as the time-dependent current under control conditions minus the time-dependent current in the presence of Ba<sup>2+</sup>, divided by the time-dependent current under control conditions. Block showed minimal time dependence, suggesting that

**Figure 2. Effects of cation substitution and [K<sup>+</sup>]<sub>o</sub> modulation on *I*<sub>KH</sub>**

A, tail currents recorded at repolarization to –40 mV after hyperpolarization to negative potentials (voltage protocol in inset) showed contamination by *I*<sub>Na</sub> activated upon depolarization from negative test potentials back to the holding potential of –40 mV. Recordings upon returning to –40 mV after a hyperpolarization to –140 mV in one cell are shown before (□) and after (■) substitution of extracellular sodium with Tris-HCl. Removal of Na<sup>+</sup> eliminated the fast inward Na<sup>+</sup> transient but did not affect the tail current. B, tail currents recorded in Na<sup>+</sup><sub>o</sub>-free solution, normalized to values at test potential of –140 mV. Half-activation voltage obtained with Boltzmann fits to normalized tail currents was –93.1 ± 4.6 mV, slope factor –15.2 ± 2.2 (*n* = 5 cells). C and D, removal of external sodium did not affect time-dependent inward *I*<sub>KH</sub>. A family of recordings obtained in the same cell with test pulses to –120, –100, –90 and –80 mV before (C) and after (D) substitution of NaCl by equimolar Tris-HCl is shown (similar results were obtained in 5 PV cardiomyocytes). E, determination of tail current reversal (voltage protocol in inset) at various external K<sup>+</sup> concentrations. The reversal potential became more positive as [K<sup>+</sup>]<sub>o</sub> increased. Linear regression (○) yielded a shift in mean *E*<sub>rev</sub> of 55.7 ± 2.4 mV decade<sup>–1</sup> change in [K<sup>+</sup>]<sub>o</sub>, with a correlation coefficient of 0.99 (*n* = 4), and was in agreement with the prediction by the Nernst equation (37°C) for a K<sup>+</sup> conductance (61.5 mV decade<sup>–1</sup>, ●). Examples of recordings before (F) and after (G) removal of external K<sup>+</sup> in the same cell are shown, with K<sup>+</sup> removal eliminating *I*<sub>KH</sub> in this and 2 other cells tested. Removal of internal K<sup>+</sup> and equimolar substitution with Cs<sup>+</sup> (20 mM CsCl and 110 mM CsAsp) led to disappearance of the outward tail currents (*n* = 3, H). [K<sup>+</sup>]<sub>o</sub>, external potassium concentration; TP, test potential.



the difference in  $IC_{50}$  between instantaneous and time-dependent current is more likely to be due to intrinsic differences in sensitivity of different currents to block by  $Ba^{2+}$  than to a time-dependent blocking mechanism. Figure 3D shows the response of instantaneous current and  $I_{KH}$  to  $Cs^+$ . Both were highly and equally sensitive: at  $-120$  mV,  $IC_{50}$  values averaged  $139.0 \pm 34.2$  versus  $184.0 \pm 18.2 \mu M$  for instantaneous and time-dependent current, respectively ( $n = 6$  cells each,  $P = n.s.$ ).

### Response to pharmacological interventions

Isoproterenol was applied extracellularly at concentrations of 10, 100 and 1000 nM. Figure 4A shows the effect of  $1 \mu M$  isoproterenol on  $I_{KH}$  in a PV cell. A clear and reversible increase was seen, with steady-state effects achieved rapidly (within 2 min). Mean current

density at  $-100$  mV increased from  $-0.9 \pm 0.1$  pA pF $^{-1}$  (control) to  $-1.2 \pm 0.1$  pA pF $^{-1}$  in the presence of 10 nM isoproterenol,  $-1.4 \pm 0.2$  pA pF $^{-1}$  with 100 nM isoproterenol and  $-1.5 \pm 0.1$  pA pF $^{-1}$  with 1000 nM isoproterenol ( $n = 14$  cells,  $P < 0.05$  versus control for each concentration). Washout returned mean current amplitude to  $-0.9 \pm 0.2$  pA pF $^{-1}$ . Mean percentage changes from baseline at each isoproterenol concentration and upon washout are shown for PV cells in Fig. 4B. Isoproterenol also had concentration-dependent effects on holding current, which increased from  $44 \pm 11$  pA pF $^{-1}$  under control conditions to  $65 \pm 14$  pA pF $^{-1}$  ( $59 \pm 14\%$  increase) at 10 nM isoproterenol,  $70 \pm 13$  pA pF $^{-1}$  ( $89 \pm 33\%$  increase) at 100 nM isoproterenol and  $87 \pm 14$  pA pF $^{-1}$  ( $144 \pm 37\%$  increase) at 1000 nM ( $P < 0.05$  versus control for all). Holding current changes were also reversible after washout.

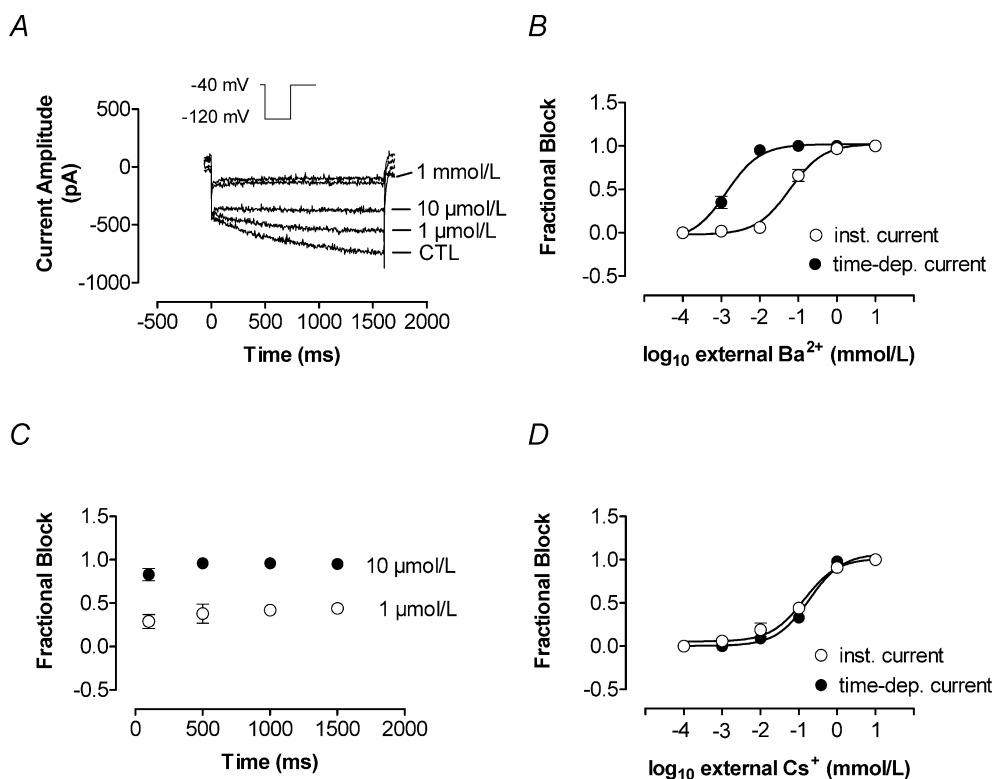


**Figure 3.**  $I_{KH}$  response to external  $Ba^{2+}$  and  $Cs^+$

Concentration-dependent inhibition of instantaneous and time-dependent current components by  $Ba^{2+}$  and  $Cs^+$ . A, representative example of the effect of  $Ba^{2+}$  on the time-dependent and instantaneous current recorded in a PV cardiomyocyte (voltage protocol in inset). The time-dependent current was exquisitely  $Ba^{2+}$  sensitive. Concentrations used were 1, 10, 100  $\mu M$  and 1 mM. B, concentration-response curves were well fitted with Hill functions, with mean  $IC_{50}$  for  $Ba^{2+}$  block at  $-120$  mV averaging  $76.0 \pm 17.9$  versus  $2.0 \pm 0.3 \mu M$  ( $n = 8$ ,  $P < 0.01$ ) for instantaneous and time-dependent current, respectively. C, mean  $\pm$  s.e.m. fractional inhibition of the time-dependent current by  $Ba^{2+}$  analysed at various time intervals during a test pulse showed only minimal time dependence of  $Ba^{2+}$  block. D, there was no significant difference between potency of  $Cs^+$  for inhibition of time-dependent versus instantaneous components ( $IC_{50}$  at  $-120$  mV:  $139 \pm 0.1$  versus  $184 \pm 1.8 \mu M$ ,  $n = 6$ ,  $P = n.s.$ ). CTL, control; inst., instantaneous component; time-dep., time-dependent component.

The inward rectification of  $I_{KH}$  led us to consider the possibility that it might be related to cholinergic  $K^+$  current, and we therefore tested its response to the muscarinic agonist carbachol. Carbachol ( $1 \mu\text{M}$ ) strongly increased both instantaneous and time-dependent current, as illustrated by the response of a PV cell illustrated in Fig. 4C. Mean time-dependent  $I_{KH}$  density–voltage relations recorded before and after carbachol in nine PV cells are shown in Fig. 4D. Carbachol increased  $I_{KH}$  by an average of  $188 \pm 54\%$  at voltages between  $-120$  and  $-90$  mV.  $I_{KH}$  in both PV and LA cells responded to carbachol (e.g. currents at  $-120$  mV increased to  $-5.0 \pm 0.6$  and  $-4.9 \pm 1.1$  pA pF $^{-1}$  from  $-2.6 \pm 0.5$  and  $-1.9 \pm 0.4$  pA pF $^{-1}$  in PV and LA, respectively,  $P < 0.01$  versus baseline,  $n = 9$  cells each). Blockade of muscarinic receptors with 200 nM atropine completely abolished the effect of carbachol (data not shown). Atropine itself had no effect on  $I_{KH}$  in the absence of carbachol.

In view of the response to carbachol, we considered the possibility that channels composed of Kir3 subunits carry  $I_{KH}$ . Tertiapin-Q is a 22-amino acid peptide synthesized from honeybee venom that blocks Kir3-based

currents at nanomolar concentrations without affecting Kir2 currents (Jin & Lu, 1999), and has been found to block acetylcholine-dependent current in the heart in a highly selective fashion (Drici *et al.* 2000). Figure 5 shows a family of currents recorded in a PV cardiomyocyte under control conditions (A) and after exposure to 200 nM tertiapin-Q (B). The inhibitory effect was completely reversible upon washout of the drug (data not shown). Tertiapin-Q completely and reversibly abolished time-dependent  $I_{KH}$ . Figure 5C shows mean current–voltage relations for the time-dependent component of the current in seven PV cardiomyocytes before and after tertiapin-Q. Whereas the time-dependent current was eliminated after  $1 \mu\text{M}$  tertiapin-Q application, mean instantaneous current decreased by  $\sim 25\%$ , a change that was not statistically significant. These data indicate that the time-dependent component is entirely tertiapin-Q sensitive, whereas a statistically non-significant minority of the instantaneous current is blocked by tertiapin-Q, supporting the notion that the instantaneous component is largely carried by a conductance (probably  $I_{K1}$ ) that is distinct from  $I_{KH}$ . Mean concentration–response data for the effect of tertiapin-Q

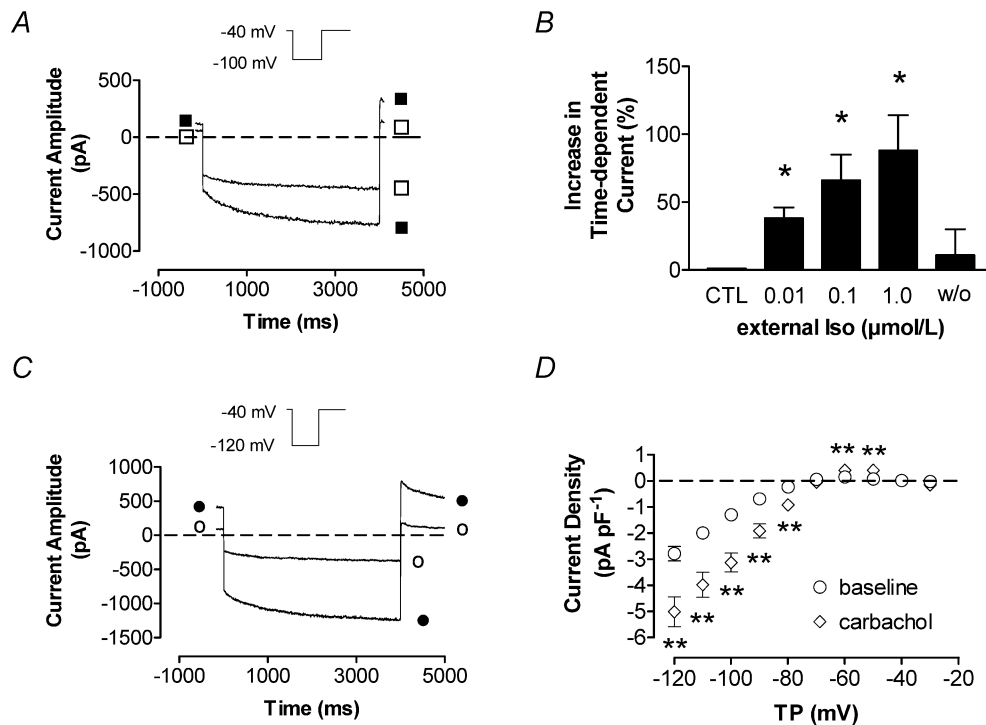


**Figure 4. Neurohumoral modulation of  $I_{KH}$**

A, representative recording from a PV cardiomyocyte after  $1 \mu\text{M}$  isoproterenol (Iso, ■) in comparison to pre-isoproterenol control (□). B, steady-state effects of Iso (after 2 min) on  $I_{KH}$  are shown as relative increases. Maximal increase in current amplitude was  $88 \pm 26\%$  by  $1 \mu\text{M}$  Iso ( $n = 14$ ,  $P < 0.01$  versus CTL). C, representative currents recorded with a pulse to  $-120$  mV before (○) and 2 min after (●) exposure to  $1 \mu\text{M}$  carbachol in one cardiomyocyte. D, mean  $\pm$  s.e.m.  $I_{KH}$ –V relationship before and after  $1 \mu\text{M}$  carbachol in 9 PV cardiomyocytes.  $**P < 0.01$  versus baseline. TP, test potential; CTL, control; w/o, washout; Iso, isoproterenol.

on time-dependent  $I_{KH}$  at  $-120$  mV in four PV cardiomyocytes are shown in Fig. 5D, and provide an  $IC_{50}$  of  $10 \pm 2$  nM, close to the reported  $IC_{50}$  for Kir 3.1/3.4 currents of 8 nM (Jin & Lu, 1999).

Having shown this effect of tertiapin-Q on  $I_{KH}$ , we repeated the application of  $1 \mu M$  isoproterenol in the presence of 200 nM tertiapin-Q in order to evaluate the potential contribution of currents other than  $I_{KH}$  (such as  $I_f$ ) to the enhancement of time-dependent hyperpolarization-activated current. In the presence of tertiapin-Q, isoproterenol failed to elicit significant hyperpolarization-activated current. For example, mean end-pulse current at  $-120$  mV averaged  $-2.84 \pm 0.89$  pA pF $^{-1}$  before tertiapin-Q in 4 cells,

versus  $0.09 \pm 0.01$  pA pF $^{-1}$  ( $P < 0.05$ ) after tertiapin-Q and  $0.20 \pm 0.07$  pA pF $^{-1}$  in the same cells in the presence of tertiapin-Q and isoproterenol ( $P = n.s.$  versus pre-isoproterenol).

### Role of $I_{KH}$ in AP repolarization

Given the high selectivity of tertiapin-Q for Kir3 channels and its potent inhibition of  $I_{KH}$ , we evaluated the effect of tertiapin-Q on repolarization of LA and PV APs in multicellular canine atrial preparations in the presence of 200 nM atropine to prevent any contribution of endogenously released acetylcholine. Figure 5E and F show representative APs before and after 100 nM tertiapin-Q in LA and PV. Mean AP duration characteristics are provided

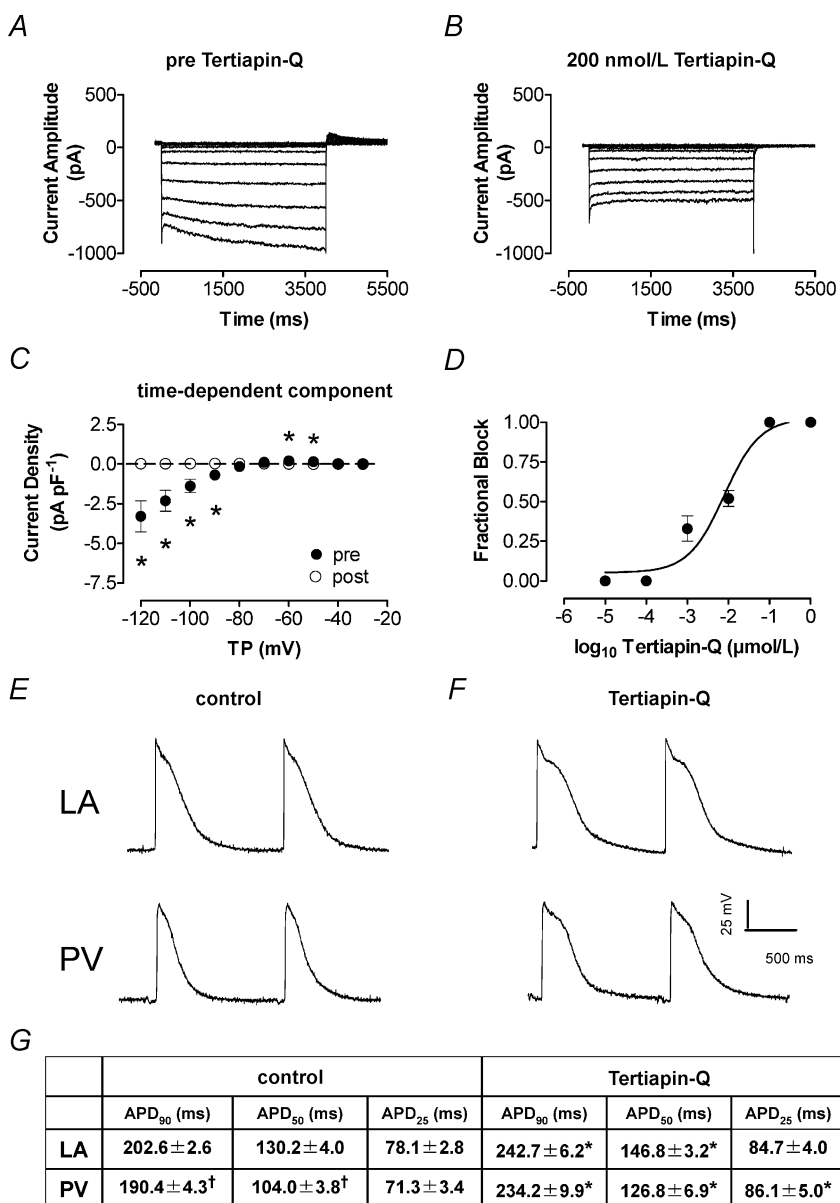


**Figure 5. Effect of tertiapin-Q on  $I_{KH}$  and action potentials**

Representative recordings (A and B) were obtained in the same cardiomyocyte. Currents recorded before (A) and after (B) application of 200 nM tertiapin-Q are shown. The inhibitory effect was reversible (not shown). C, effect of tertiapin-Q on the time-dependent current component ( $n = 7$  cells). Mean  $\pm$  S.E.M.  $I_{KH}$  density is shown prior to (pre) and during (post) tertiapin-Q exposure ( $*P < 0.05$ ). D, Hill fit to mean  $\pm$  S.E.M. fractional block at increasing concentrations of tertiapin-Q, providing an  $IC_{50}$  of  $10 \pm 2.1$  nM ( $n = 4$ ). E and F, representative APs from LA and PV cardiomyocytes recorded with standard microelectrode techniques in coronary perfused multicellular tissue preparations. E and F, APs recorded under control conditions (in the presence of 200 nM atropine) (E) and APs after the application of 100 nM tertiapin-Q (F) (all recordings at 2 Hz in the presence of 200 nM atropine). G shows mean  $\pm$  S.E.M. AP duration in 25 LA and 29 PV cells studied under control conditions and 12 LA, 11 PV cells after tertiapin-Q. APD = AP duration at 2 Hz. TP, test potential; APD<sub>90</sub>, APD<sub>50</sub>, APD<sub>25</sub>, APD to 90, 50 and 25% repolarization, respectively,  $*P < 0.05$  versus control,  $\dagger P < 0.05$  versus LA.



in the table at the bottom of Fig. 5, and indicate that tertiapin-Q significantly prolonged AP duration in both regions.

### Potential role of G proteins in $I_{KH}$ regulation

In the light of a possible contribution of Kir3 channels to  $I_{KH}$  current, we studied the effects of a variety of interventions targeting G proteins. In each case, experiments were performed in one cell under control conditions followed by another cell from the same batch studied in the presence of an intervention, in order to exclude data contamination by inter-day and inter-isolate differences in  $I_{KH}$  amplitude and response. When GTP was not included in the pipette solution, basal  $I_{KH}$  was not altered. However, in the absence of pipette GTP the addition of carbachol failed to further activate  $I_{KH}$  (Fig. 6A and B). For example, at  $-120$  mV current density in cells patched with GTP-free pipettes averaged  $-8.3 \pm 0.7$  versus  $-8.3 \pm 1.1$  pA pF $^{-1}$  ( $P = \text{n.s.}$ ,  $n = 4$ ) before and after  $1 \mu\text{M}$  carbachol, respectively. In the same batches of cells studied on the same days with GTP-containing pipettes,  $I_{KH}$  increased from  $-6.2 \pm 1.0$  to  $-10.0 \pm 1.2$  pA pF $^{-1}$  ( $P < 0.05$ ,  $n = 4$ ) upon exposure to carbachol.

We next sought to examine the effect of substituting the non-hydrolysable analogue GTP $\gamma$ S for GTP in the pipette. As illustrated in Fig. 6C and D, the inclusion of GTP $\gamma$ S significantly increased  $I_{KH}$  in the absence of cholinergic stimulation compared to current recorded with pipettes containing regular GTP (e.g. at  $-120$  mV from  $-3.8 \pm 0.6$  to  $-8.2 \pm 0.8$  pA pF $^{-1}$ ,  $P < 0.05$ ,  $n = 6$  cells each). In addition, GTP $\gamma$ S fully prevented any further  $I_{KH}$  response to carbachol, suggesting that  $I_{KH}$  was already maximally activated in the presence of GTP $\gamma$ S.

Preincubation with  $1.5 \text{ mg l}^{-1}$  PTX also attenuated the effect of carbachol (Fig. 6E and F). For example, at  $-120$  mV carbachol increased  $I_{KH}$  density from  $-6.2 \pm 1.8$  to  $-11.5 \pm 1.8$  pA pF $^{-1}$  in cells incubated without PTX at  $37^\circ\text{C}$  for  $>9$  h ( $P < 0.05$  for carbachol effect,  $n = 6$ ). In cells preincubated with PTX at the same temperature and time,  $I_{KH}$  density averaged  $-6.4 \pm 0.8$  pA pF $^{-1}$  before carbachol and  $-5.5 \pm 1.2$  pA pF $^{-1}$  in the presence of carbachol at  $-120$  mV ( $P = \text{n.s.}$ ,  $n = 6$ ). The response of  $I_{KH}$  tail current to carbachol was significantly reduced in PTX-treated cells, but not abolished. For example, following hyperpolarization to  $-120$  mV tail currents averaged  $2.1 \pm 0.7$  and  $8.4 \pm 1.6$  pA pF $^{-1}$  ( $P < 0.01$ ) before and after carbachol under PTX-free conditions and  $1.8 \pm 0.6$  and  $3.4 \pm 0.9$  pA pF $^{-1}$  ( $P < 0.01$ ) before and after carbachol in PTX-preincubated cells ( $n = 6$  for each).

Overall, carbachol increased  $I_{KH}$  tail currents following a pulse to  $-120$  mV by  $538 \pm 170\%$  in cells incubated without PTX versus  $127 \pm 37\%$  ( $P < 0.05$  versus change in absence of PTX) in PTX-treated cells.

### Potential role of $I_{KH}$ in atrial tachycardia-induced remodelling

Figure 7A shows mean  $\pm$  s.e.m.  $I_{KH}$  density–voltage relations in control dogs and dogs subjected to 7 day atrial tachycardia (AT) for LA and PV cardiomyocytes.  $I_{KH}$  was increased modestly in LA cardiomyocytes. Larger increases in  $I_{KH}$  were seen in PV cells.

$I_{KH}$  was not significantly affected by AT remodelling when measured in the presence of  $1\text{-}\mu\text{M}$  carbachol (Fig. 7B), in contrast to the up-regulation observed in the absence of carbachol (Fig. 7A). These results suggest that maximally available  $I_{KH}$  is similar in the absence versus presence of AT remodelling, and that regulatory factors may explain the differences observed in the absence of cholinergic stimulation. Similarly, in the presence of  $1 \mu\text{M}$  carbachol, time-dependent  $I_{KH}$  densities were not significantly different between control LA and PV cells (Fig. 7C), in contrast to the higher PV  $I_{KH}$  density in the absence of carbachol, again consistent with a prime role for regulatory factors in the PV–LA  $I_{KH}$  difference. In contrast, the instantaneous component recorded in the presence of  $1 \mu\text{M}$  carbachol was significantly reduced by AT remodelling in both LA and PV cells (Fig. 7D).

### Possible molecular basis for $I_{KH}$

The expression of Kir3.1, 3.2 and 3.4 channel subunits was evaluated in isolated LA and PV cardiomyocytes with Western blot and semiquantitative immunohistochemical methods. Immunohistochemical studies confirmed the presence of Kir3.1 and 3.4 on isolated LA and PV cardiomyocytes, with clear membrane staining (Fig. 8A and B). Kir3.2 staining was fainter and no outer membrane distribution was observed (Fig. 8C). Quantitative analysis of immunofluorescence indicated no significant differences between LA and PV cardiomyocytes in Kir3 subunit immunofluorescence intensity (right panels). Kir3 subunit expression as measured by Western blotting of isolated cardiomyocyte membrane preparations was not significantly different in LA versus PV (Fig. 9A and B). Atrial tachypacing reduced Kir3.4 expression, but did not significantly affect Kir3.1.  $M_2$  muscarinic receptor and inhibitory G protein ( $G_{\alpha i}$ ) expression was down-regulated by atrial

tachycardia-induced remodelling (Figs 9C and D), consistent with the decreased response of the instantaneous component to carbachol shown in Fig. 7C.

## Discussion

### Major findings

We characterized in detail a time-dependent inwardly rectifying  $K^+$ -current,  $I_{KH}$ , in canine atrial cardiomyocytes.  $I_{KH}$  sensitivity to  $Ba^{2+}$  is instantaneous rather than time dependent, favouring conductance by Kir3

channels over Kir2 (Yamada *et al.* 1998).  $I_{KH}$  sensitivity to tertiapin-Q resembles that seen with Kir3.1/3.4 channels (Jin & Lu, 1999), pointing to possible constitutive, agonist-independent Kir3.1/3.4 activity.  $I_{KH}$  is subject to modulation by important endogenous neurotransmission systems (adrenergic and cholinergic), and by a recognized atrial arrhythmogenic intervention (atrial tachycardia-induced remodelling).

### Possible molecular basis

$I_{KH}$  is an inwardly rectifying, highly  $K^+$ -selective conductance sensitive to  $Ba^{2+}$ , properties compatible with

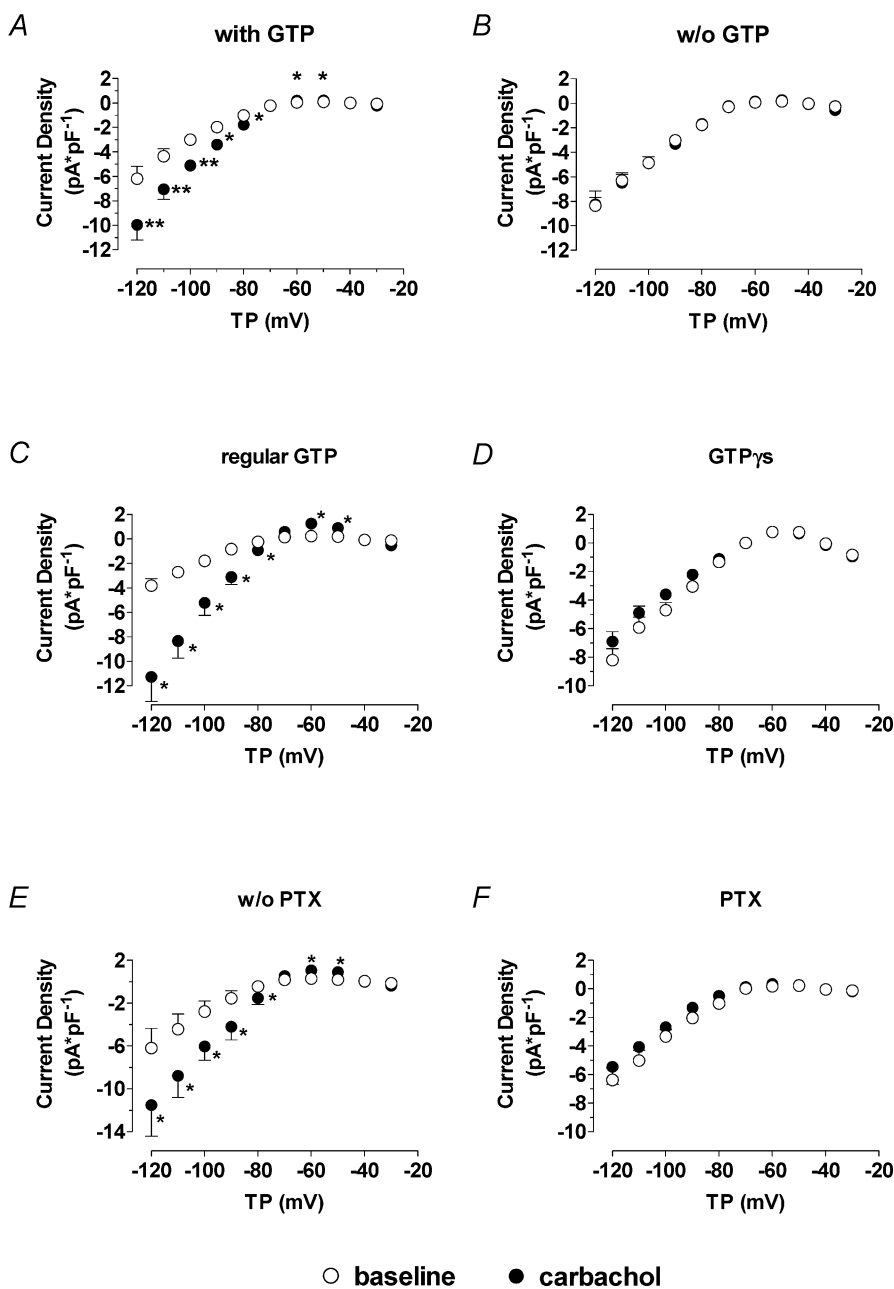


**Figure 6. Elements of G protein signalling pathways affect  $I_{KH}$**

A and B indicate mean  $\pm$  S.E.M.  $I_{KH}$ -voltage relationships recorded from 4 cells each before and after external application of  $1 \mu M$  carbachol with (A) and without (B) GTP in the internal solution. C and D, inclusion of intracellular GTP $\gamma$ S ( $0.1 \text{ mM}$ ) in place of regular GTP increased baseline  $I_{KH}$  and prevented further carbachol-induced ( $1 \mu M$ ) activation. Mean  $\pm$  S.E.M. current-voltage relationships for 6 experiments each with GTP-containing (C) and with GTP $\gamma$ S-containing (D) pipettes. E and F, PTX effects: cardiomyocytes ( $n = 6$ ) were preincubated with ( $F$ )  $1.5 \text{ mg l}^{-1}$  pertussis toxin (PTX) for 9 h. Control recordings were performed in 6 cells from the same isolates incubated for the same period but without external PTX (E). Preincubation with PTX prevented carbachol enhancement of  $I_{KH}$ . Results are mean  $\pm$  S.E.M. current-voltage relationships. \* $P < 0.05$ , \*\* $P < 0.01$ ; TP, test potential; w/o, without; PTX, pertussis toxin.

several inward-rectifying Kir subunits. Tertiapin-Q is a highly selective inward-rectifier K<sup>+</sup> channel blocker that inhibits Kir1 channels with an IC<sub>50</sub> of 2 nM and Kir3.1/3.4 with an IC<sub>50</sub> of 8 nM, but has minimal effects on Kir2.1 channels at micromolar concentrations (Jin & Lu, 1999). Acetylcholine-dependent K<sup>+</sup> current (*I*<sub>KACH</sub>) in native cells, based on Kir3.1 and 3.4 subunit heteromers, is suppressed by tertiapin-Q with IC<sub>50</sub> values ranging from 8 to 30 nM (Drici *et al.* 2000; Kitamura *et al.* 2000), concentrations with no effect on *I*<sub>Kr</sub>, *I*<sub>Ks</sub>, *I*<sub>to</sub>, *I*<sub>K1</sub> or *I*<sub>KATP</sub> (Drici *et al.* 2000; Kitamura *et al.* 2000). The action of tertiapin-Q on *I*<sub>KACH</sub> is independent of muscarinic receptor activation state (Yamada, 2002). *I*<sub>KH</sub>-like kinetics have been noted for *I*<sub>KACH</sub> in human atrial myocytes (Heidbuchel *et al.* 1987) and Kir3.1/3.4 channels activated by Gβγ subunits (Reuveny *et al.* 1994). Kir1.1 subunits carry tertiapin-sensitive currents (Jin & Lu, 1999) and are detectable in PV cardiomyocytes (Michelakis *et al.* 2001); however, Kir1-based currents lack *I*<sub>KH</sub> kinetics (Schuck *et al.* 1994) and are more sensitive to tertiapin-Q than Kir3 current (Jin & Lu, 1999), *I*<sub>KACH</sub> (Drici *et al.* 2000; Kitamura *et al.* 2000) or *I*<sub>KH</sub>. All of these observations suggest that *I*<sub>KH</sub> is carried by constitutive Kir3 subunit activity.

PV expression of Kir3.1 and Kir3.4 proteins was not different from LA (Figs 8 and 9), suggesting that larger PV *I*<sub>KH</sub> may be due to regulatory factors, rather than differences in ion channel expression. Signalling events besides direct Gβγ modulation of Kir3 channels may be important for determining basal and agonist-stimulated current (Yamada *et al.* 1998). Kir3-channel activity is increased by protein kinase A (PKA) and inhibited by phosphatases (Mullner *et al.* 2000). Phosphatidylinositol phosphates increase current through Kir3 channels and are regulated by Gq-mediated signalling (Kobrinisky *et al.* 2000). Channel activity is regulated by intracellular sodium and chloride (Mirshahi *et al.* 2003) and by extracellular and intracellular pH (Mao *et al.* 2003). Stretch also inhibits Kir3 channels (Zhang *et al.* 2003). Ca<sup>2+</sup>-calmodulin facilitates GTPase activity of regulators of G protein signalling (RGS) proteins by suppressing inhibitory effects of phosphatidylinositol-3,4,5-trisphosphate (PIP<sub>3</sub>) on RGS4 activity (Ishii *et al.* 2002). G protein-regulated K<sup>+</sup> currents showed time dependence like *I*<sub>KH</sub>, suggesting that similar complex lipid-protein interactions may regulate *I*<sub>KH</sub> kinetics and function. Such regulation may be important in maintaining basal *I*<sub>KH</sub>

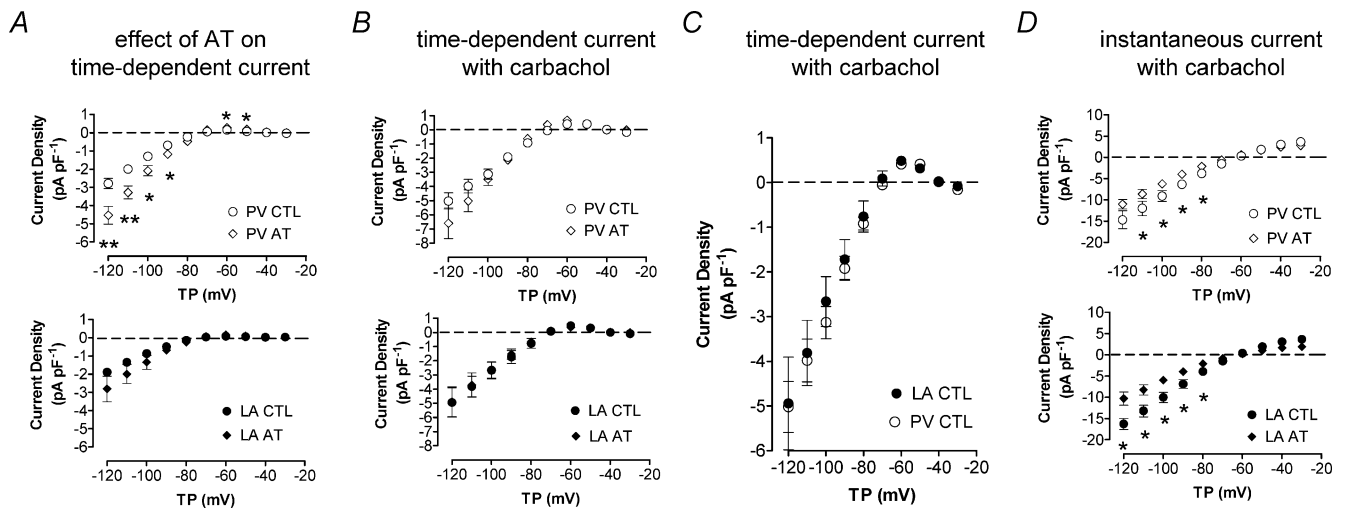


**Figure 7. Atrial tachycardia-induced changes and modulation by carbachol**

A, mean  $\pm$  s.e.m. *I*<sub>KH</sub>-voltage relations for PV (top panel) and LA (bottom panel) cells, for 27 PV cells from 14 control dogs and 9 cells from 6 atrial-tachypaced (AT, 400 beats min<sup>-1</sup> for 1 week) dogs and 26 LA cells from 13 control dogs and 12 cells from 6 AT dogs. Top panels of B and D compare mean *I*-*V* curves in the presence of 1  $\mu$ M carbachol for the time-dependent and instantaneous components, respectively, in PV myocytes from control and AT dogs (*n* = 9 cells/group). There was no difference in the time-dependent component, whereas the instantaneous component was significantly reduced by AT. Bottom panels of B and D show mean data for LA cardiomyocytes (8 and 12 cells, respectively) in the same format as top panels. C, mean  $\pm$  s.e.m. *I*<sub>KH</sub>-voltage relationship (time-dependent component) of 9 PV and 7 LA cardiomyocytes exposed to 1  $\mu$ M carbachol (*P* = n.s., all cells from control dogs). There was no difference in carbachol-induced currents between LA and PV cells. TP, test potential; CTL, control; AT, atrial tachycardia; \**P* < 0.05, \*\**P* < 0.01 versus CTL.

activity, as neither PTX nor absence of GTP affected  $I_{KH}$  in the absence of carbachol. Alterations in these signalling pathways may occur during atrial tachypacing and may lead to increased basal  $I_{KH}$ . Further experiments are needed to define the exact mechanisms of  $I_{KH}$  regulation.

### Relationship to previous studies

Chen *et al.* (2001) observed time-dependent inward currents upon hyperpolarization of PV cardiomyocytes, and believed them to be  $I_f$ . These currents may correspond to  $I_{KH}$ ; however, since they were not characterized in the Chen study, it is impossible to be sure. Dobrev *et al.* (2001) noted  $I_{KACH}$  down-regulation in atrial myocytes from patients with AF. Kir3.4 mRNA levels were reduced, but protein expression was not assayed. We observed decreased  $M_2$  receptor and  $G_i$  protein expression with atrial tachycardia-induced remodelling, which could account for  $I_{KACH}$  down-regulation. We also saw slight decreases in Kir3.4, but not Kir3.1, protein expression with atrial tachycardia-induced remodelling.

Many properties of  $I_{KH}$  suggest that it is carried by constitutively active  $I_{KACH}$  channels. Evidence for constitutive  $I_{KACH}$  channel activity in cardiomyocytes has been presented by Heidbuchel *et al.* (1992a,b). The lack

of change in baseline  $I_{KH}$  with GTP-free pipettes indicates that the constitutively active, time-dependent current does not require intracellular GTP under basal conditions. However, an important role for G protein regulation is indicated by the maximally increased current upon inclusion of GTP $\gamma$ S in the pipette. The attenuation of the carbachol response by PTX preincubation and its abolition in the presence of GTP-free or GTP $\gamma$ S-containing pipette solutions indicates that the signal transduction pathway coupling muscarinic receptor stimulation to  $I_{KH}$  requires PTX-sensitive G proteins.

### Potential significance

Tertiapin-Q prolonged AP duration recorded with standard microelectrode techniques from multicellular LA and PV preparations in the presence of atropine to exclude contributions from endogenous acetylcholine, pointing to a potentially significant role for  $I_{KH}$  in LA and PV cardiomyocyte repolarization. Since atrial tachycardia-induced remodelling increases  $I_{KH}$ , it may contribute to AF-promoting action potential abbreviation caused by persistent atrial tachyarrhythmias (Yue *et al.* 1997; van der Velden *et al.* 2000).

The autonomic nervous system (parasympathetic and sympathetic) is known to contribute to atrial

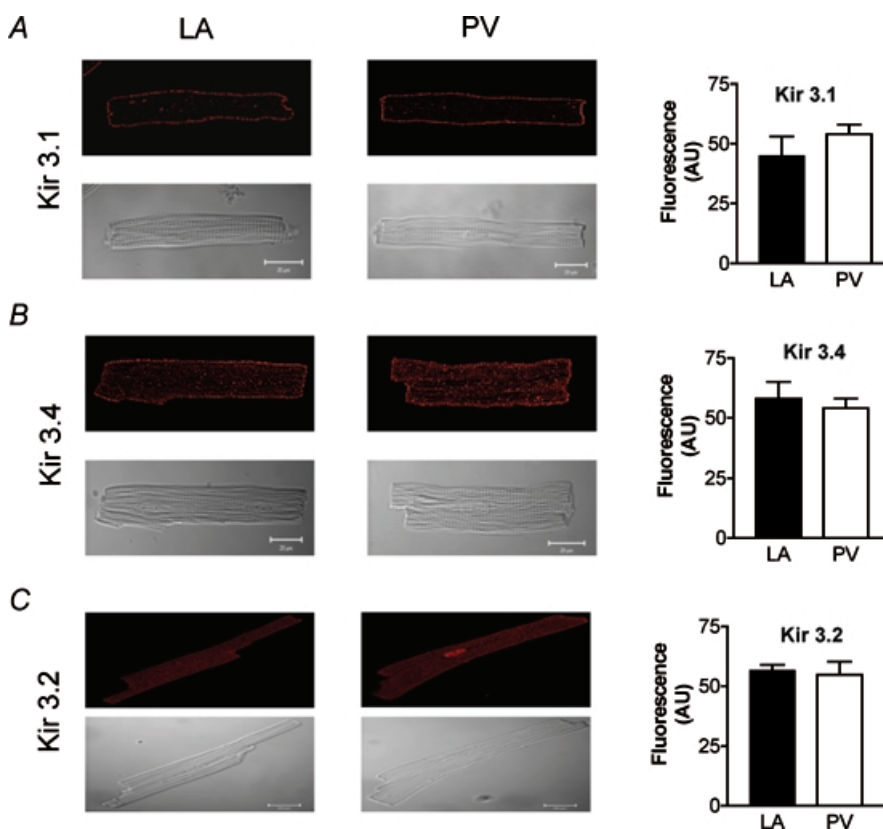


**Figure 8. Immunofluorescence studies**

Top of each panel shows representative deconvoluted confocal images of native cardiomyocytes from LA and PV probed with anti-Kir 3.1 (A), anti-Kir 3.4 (B) and anti-Kir 3.2 (C) antibody and TRITC-conjugated anti-rabbit secondary antibody (red). Both anti-Kir 3.1 and anti-Kir 3.4 antibodies stained cells at the outer membrane, and anti-Kir 3.4 also stained T-tubular structures. Kir 3.2 was predominantly located at the T-tubules and staining was weaker than for the other subunits. Bottom of each panel shows phase-contrast microscopy of the same cell(s). Right side: mean whole-cell fluorescence levels were similar between regions for all subunits. Outer membrane fluorescence for anti-Kir 3.4 and 3.1 staining was also similar between PV and LA cardiomyocytes (data not shown). AU, arbitrary units.

arrhythmogenesis.  $\beta$ -Adrenergic stimulation hyperpolarizes atrial myocytes (Boyden *et al.* 1983); however, isoproterenol typically inhibits  $I_{K1}$  (Koumi *et al.* 1995; Zhang *et al.* 2002). The increase in  $I_{KH}$  caused by  $\beta$ -adrenergic stimulation shown here is a potential contributor to AF promotion and atrial myocyte hyperpolarization resulting from adrenergic stimulation.  $I_{KH}$  is also a candidate to participate in cholinergic AF promotion. Atrial tachycardia-induced remodelling is a significant factor in clinical AF (Nattel, 2002). Ionic current changes that may contribute to remodelling-induced APD-abbreviation include decreased  $I_{Ca}$  and increased  $I_{K1}$  (Yue *et al.* 1997; Bosch *et al.* 1999; Dobrev *et al.* 2001). The present findings add  $I_{KH}$  up-regulation as a potential contributor to atrial-tachycardia induced APD abbreviation. The larger  $I_{KH}$  in PV *versus* LA cells after tachycardia-induced remodelling (Fig. 7) suggests that  $I_{KH}$  may contribute to the role of PVs in AF maintenance (Wu *et al.* 2001).

Our study suggests that  $\beta$ -adrenoceptor activation can stimulate Kir3-based channels in cardiomyocytes. Kir3 channels are opened by the  $G\beta\gamma$  heterodimer in response to  $G_i$  activation by  $M_2$  muscarinic receptors (Lim *et al.* 1995). It was believed that  $\beta$ -adrenoceptors were incapable of modulating these currents in native tissues (Trautwein *et al.* 1982). Some investigators found an increase in  $I_{KACH}$  with isoproterenol application (Kim, 1990; Sorota *et al.* 1999; Mullner *et al.* 2000). Others attributed the effect of isoproterenol on  $I_{KACH}$  to isoproterenol-activated  $I_{K,ATP}$  (Wang & Lipsius, 1995). The present study suggests that  $\beta$ -adrenoceptor stimulation of Kir3-based current occurs in LA and PV cells, and that the organization of signalling may therefore be cell-type dependent.

### Potential limitations

We defined  $I_{KH}$  based on the slowly activating time-dependent current component. The complete

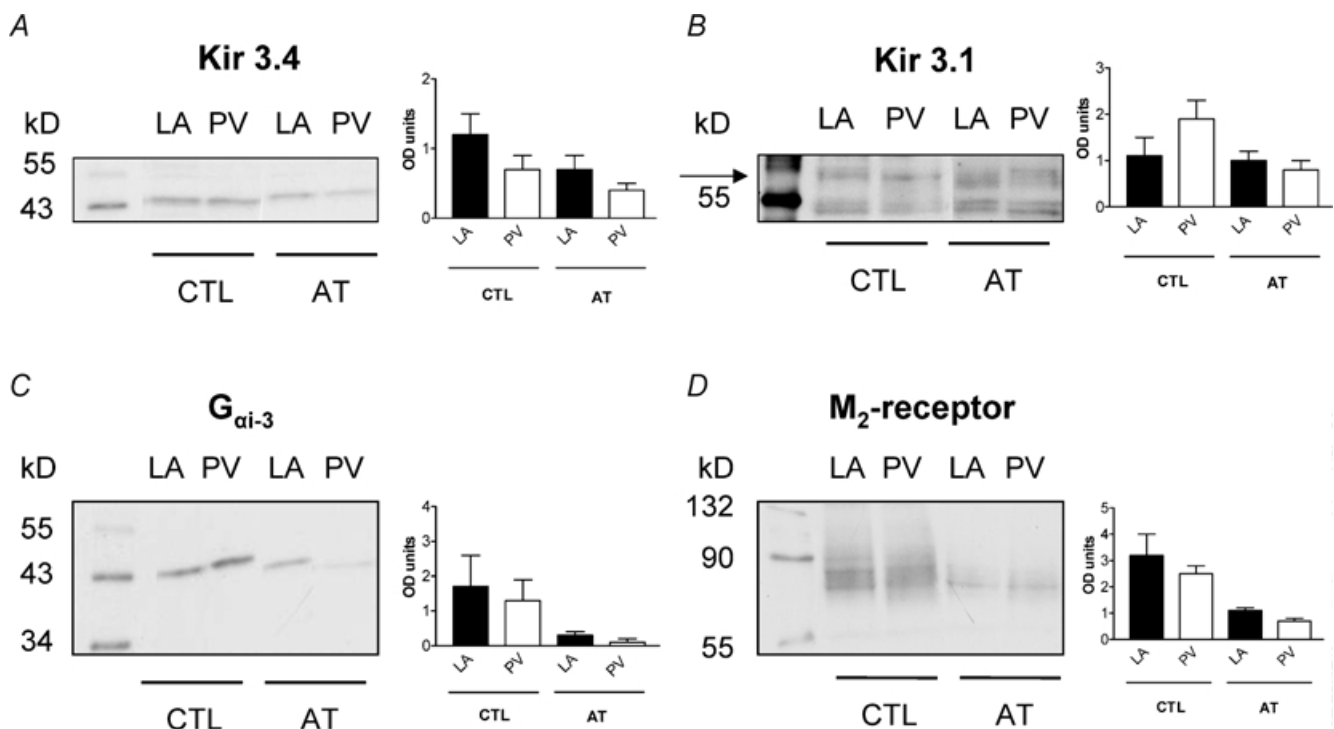


**Figure 9. Immunoblots for Kir3 subunits,  $M_2$  receptor and  $G_{\alpha i}$**

Representative bands obtained by Western blots for LA and PV cardiomyocyte crude membrane preparations under control conditions (CTL, left of each panel) and after atrial tachycardia (AT, right). Mean  $\pm$  s.e.m. optical density of the bands after normalization to GAPDH content of each individual lane on the membrane is shown at the right side of the panel. A, blotting of crude membrane extracts with anti-Kir 3.4 antibody yielded bands indicative of channel monomers (~48 kDa). Mean optical densities were not significantly different between the 2 regions. B, blotting with anti-Kir 3.1 antibody yielded bands at ~58 kDa compatible with Kir 3.1 core protein (specificity confirmed by preincubation with control antigen) and was also unchanged by AT. C and D representative results of blots with anti- $G_{\alpha i-3}$  antibody (~45 kDa) and anti- $M_2$  receptor antibody (~65 kDa) show no differences between the two regions but a reduction of optical densities in AT. CTL, control; AT, atrial tachycardia; OD, optical density.

abolition of this time-dependent component by tertiapin-Q justifies its consideration as a distinct entity. In some experiments, we contrasted the time-dependent  $I_{KH}$  component with instantaneous current. The instantaneous component is carried largely by  $I_{K1}$ ; however, there was some evidence for a potential contribution from  $I_{KH}$ . Since tertiapin-Q produced statistically non-significant and relatively minor effects on instantaneous current, it is reasonable to contrast the latter component with the slowly activating time-dependent current; nevertheless, it must be recognized that the distinction between the components is imperfect.

While we showed  $I_{KH}$  to have properties of a Kir3-based current modulated by PTX-sensitive G proteins, many mechanistic aspects remain to be elucidated. Such issues as the basis for the large constitutive current, the fundamental mechanism of its time dependence, the detailed G protein-coupled regulation, the molecular determinants of up-regulation by atrial tachycardia and the differential expression of  $I_{KH}$  in PV and LA cardiomyocytes are important and unresolved, and need further investigation.

## References

- Bosch RF, Zeng X, Grammer JB, Popovic K, Mewis C & Kuhlkamp V (1999). Ionic mechanisms of electrical remodeling in human atrial fibrillation. *Cardiovasc Res* **44**, 121–131.
- Boyden PA, Cranefield PF & Gadsby DC (1983). Noradrenaline hyperpolarizes cells of the canine coronary sinus by increasing their permeability to potassium ions. *J Physiol* **339**, 185–206.
- Chen YJ, Chen SA, Chen YC, Yeh HI, Chan P, Chang MS & Lin CI (2001). Effects of rapid atrial pacing on the arrhythmogenic activity of single cardiomyocytes from pulmonary veins: implication in initiation of atrial fibrillation. *Circulation* **104**, 2849–2854.
- DiFrancesco D (1993). Pacemaker mechanisms in cardiac tissue. *Annu Rev Physiol* **55**, 455–472.
- Dobrev D, Graf E, Wettwer E, Himmel HM, Hala O, Doerfel C, Christ T, Schuler S & Ravens U (2001). Molecular basis of downregulation of G-protein-coupled inward rectifying  $K(+)$  current ( $I_{K(ACh)}$ ) in chronic human atrial fibrillation: decrease in GIRK4 mRNA correlates with reduced  $I_{K(ACh)}$  and muscarinic receptor-mediated shortening of action potentials. *Circulation* **104**, 2551–2557.
- Drici MD, Diochot S, Terrenoire C, Romey G & Lazdunski M (2000). The bee venom peptide tertiapin underlines the role of  $I_{K(ACh)}$  in acetylcholine-induced atrioventricular blocks. *Br J Pharmacol* **131**, 569–577.
- Ehrlich JR, Cha TJ, Zhang L, Chartier D, Melnyk P, Hohnloser SH & Nattel S (2003). Cellular electrophysiology of canine pulmonary vein cardiomyocytes: action potential and ionic current properties. *J Physiol* **551**, 801–813.
- Haissaguerre M, Jais P, Shah DC, Takahashi A, Hocini M, Quiniou G, Garrigue S, Le Mouroux A, Le Metayer P & Clementy J (1998). Spontaneous initiation of atrial fibrillation by ectopic beats originating from the pulmonary veins. *N Engl J Med* **339**, 659–666.
- Heidbuchel H, Callewaert G, Vereecke J & Carmeliet E (1992a). Activation of guinea pig atrial muscarinic  $K^+$  channels by nucleoside triphosphates in the absence of acetylcholine. *J Cardiovasc Electrophysiol* **3**, 457–473.
- Heidbuchel H, Callewaert G, Vereecke J & Carmeliet E (1992b). Membrane-bound nucleoside diphosphate kinase activity in atrial cells of frog, guinea pig, and human. *Circ Res* **71**, 808–820.
- Heidbuchel H, Vereecke J & Carmeliet E (1987). The electrophysiological effects of acetylcholine in single human atrial cells. *J Mol Cell Cardiol* **19**, 1207–1219.
- Ishii M, Inanobe A & Kurachi Y (2002). PIP3 inhibition of RGS protein and its reversal by  $Ca^{2+}$ /calmodulin mediated voltage-dependent control of the G protein cycle in a cardiac  $K^+$  channel. *Proc Natl Acad Sci U S A* **99**, 4325–4330.
- Jin W & Lu Z (1999). Synthesis of a stable form of tertiapin: a high-affinity inhibitor for inward-rectifier  $K^+$  channels. *Biochemistry* **38**, 14286–14293.
- Kim D (1990). Beta-adrenergic regulation of the muscarinic-gated  $K^+$  channel via cyclic AMP-dependent protein kinase in atrial cells. *Circ Res* **67**, 1292–1298.
- Kitamura H, Yokoyama M, Akita H, Matsushita K, Kurachi Y & Yamada M (2000). Tertiapin potently and selectively blocks muscarinic  $K(+)$  channels in rabbit cardiac myocytes. *J Pharmacol Exp Ther* **293**, 196–205.
- Kneller J, Ramirez RJ, Chartier D, Courtemanche M & Nattel S (2002). Time-dependent transients in an ionically based mathematical model of the canine atrial action potential. *Am J Physiol Heart Circ Physiol* **282**, H1437–H1451.
- Kobrinisky E, Mirshahi T, Zhang H, Jin T & Logothetis DE (2000). Receptor-mediated hydrolysis of plasma membrane messenger  $PIP_2$  leads to  $K^+$ -current desensitization. *Nature Cell Biol* **2**, 507–514.
- Koumi S, Wasserstrom JA & Ten Eick RE (1995). Beta-adrenergic and cholinergic modulation of inward rectifier  $K^+$  channel function and phosphorylation in guinea-pig ventricle. *J Physiol* **486**, 661–678.
- Li D, Fareh S, Leung TK & Nattel S (1999). Promotion of atrial fibrillation by heart failure in dogs: atrial remodeling of a different sort. *Circulation* **100**, 87–95.
- Lim NF, Dascal N, Labarca C, Davidson N & Lester HA (1995). A G protein-gated  $K$  channel is activated via beta 2-adrenergic receptors and G beta gamma subunits in *Xenopus* oocytes. *J General Physiol* **105**, 421–439.

- Mao J, Wu J, Chen F, Wang X & Jiang C (2003). Inhibition of G-protein-coupled inward rectifying K<sup>+</sup> channels by intracellular acidosis. *J Biol Chem* **278**, 7091–7098.
- Michelakis ED, Weir EK, Wu X, Nsair A, Waite R, Hashimoto K, Puttagunta L, Knaus HG & Archer SL (2001). Potassium channels regulate tone in rat pulmonary veins. *Am J Physiol Lung Cell Mol Physiol* **280**, L1138–L1147.
- Mirshahi T, Jin T & Logothetis DE (2003). G beta gamma and KACH: old story, new insights. *Sci STKE* **194**, PE32.
- Mullner C, Vorobiov D, Bera AK, Uezono Y, Yakubovich D, Frohnwieser-Steinecker B, Dascal N & Schreibleyner W (2000). Heterologous facilitation of G protein-activated K(+) channels by beta-adrenergic stimulation via cAMP-dependent protein kinase. *J General Physiol* **115**, 547–558.
- Nattel S (2002). New ideas about atrial fibrillation 50 years on. *Nature* **415**, 219–226.
- Pappone C, Rosanio S, Oreto G, Tocchi M, Gugliotta F, Vicedomini G, Salvati A, Dicandia C, Mazzone P, Santinelli V, Gulletta S & Chierchia S (2000). Circumferential radiofrequency ablation of pulmonary vein ostia. A new anatomic approach for curing atrial fibrillation. *Circulation* **102**, 2619–2628.
- Reuveny E, Slesinger PA, Inglese J, Morales JM, Iniguez-Lluhi JA, Lefkowitz RJ, Bourne HR, Jan YN & Jan LY (1994). Activation of the cloned muscarinic potassium channel by G protein beta gamma subunits. *Nature* **370**, 143–146.
- Schuck ME, Bock JH, Benjamin CW, Tsai TD, Lee KS, Slightom JL & Bienkowski MJ (1994). Cloning and characterization of multiple forms of the human kidney ROM-K potassium channel. *J Biol Chem* **269**, 24261–24270.
- Sorota S, Rybina I, Du Yamamoto A & XY (1999). Isoprenaline can activate the acetylcholine-induced K<sup>+</sup> current in canine atrial myocytes via G<sub>s</sub>-derived betagamma subunits. *J Physiol* **514**, 413–423.
- Trautwein W, Taniguchi J & Noma A (1982). The effect of intracellular cyclic nucleotides and calcium on the action potential and acetylcholine response of isolated cardiac cells. *Pflugers Arch* **392**, 307–314.
- van der Velden HMWZL, Wijffels MC, van Leuven C, Dorland R, Vos MA, Jongsma HJ & Allessie MA (2000). Atrial fibrillation in the goat induces changes in monophasic action potential and mRNA expression of ion channels involved in repolarization. *J Cardiovasc Electrophysiol* **11**, 1262–1269.
- Wang YG & Lipsius SL (1995). Beta-adrenergic stimulation induces acetylcholine to activate ATP-sensitive K<sup>+</sup> current in cat atrial myocytes. *Circ Res* **77**, 565–574.
- Wu TJ, Ong JJ, Chang CM, Doshi RN, Yashima M, Huang HL, Fishbein MC, Ting CT, Karagueuzian HS & Chen PS (2001). Pulmonary veins and ligament of marshall as sources of rapid activations in a canine model of sustained atrial fibrillation. *Circulation* **103**, 1157–1163.
- Yamada M (2002). The role of muscarinic K(+) channels in the negative chronotropic effect of a muscarinic agonist. *J Pharmacol Exp Ther* **300**, 681–687.
- Yamada M, Inanobe A & Kurachi Y (1998). G protein regulation of potassium ion channels. *Pharmacol Rev* **50**, 723–760.
- Yue L, Feng J, Gaspo R, Li GR, Wang Z & Nattel S (1997). Ionic remodeling underlying action potential changes in a canine model of atrial fibrillation. *Circ Res* **81**, 512–525.
- Yue L, Feng J, Li GR & Nattel S (1996). Transient outward and delayed rectifier currents in canine atrium: properties and role of isolation methods. *Am J Physiol* **270**, H2157–H2168.
- Zhang L, Lee JK, John SA, Uozumi N & Kodama I (2003). Mechanosensitivity of GIRK channels is mediated by PKC-dependent channel-PIP2 interaction. *J Biol Chem* **279**, 7037–7047.
- Zhang LM, Wang Z & Nattel S (2002). Effects of sustained beta-adrenergic stimulation on ionic currents of cultured adult guinea pig ventricular myocytes. *Am J Physiol Heart Circ Physiol* **282**, H880–H889.

## Acknowledgements

This work was supported by the Canadian Institutes of Health Research, the Quebec Heart and Stroke Foundation and the Mathematics of Information Technology and Complex Systems (MITACS) Network. Kir3.4 antibody was a generous gift from Dr G. Krapivinsky. The authors thank Evelyn Landry, Nathalie L'Heureux, Chantal Maltais and Chantal St-Cyr for technical assistance, France Thériault for secretarial help and Sylvain Durocher for assistance with figures. Joachim Ehrlich was a Heart and Stroke Foundation of Canada (HSFC) Research Fellow and Tae-Joon Cha is supported by a Merck Pharmacology Fellowship. Terence E. Hébert is a McDonald scholar of the HSFC.